Enhanced quantum yield of photoluminescent porous silicon prepared by supercritical drying

Joo, Jinmyoung; Defforge, Thomas; Loni, Armando; Kim, Dokyoung; Li, Z.Y.; Sailor, Michael J.; Gautier, Gael; Canham, Leigh

DOI:
10.1063/1.4947084

AIP Applied Physics Letters

Enhanced quantum yield of photoluminescent porous silicon prepared by supercritical drying

Jinmyoung Joo, Thomas Defforge, Armando Loni, Dokyoung Kim, Z. Y. Li, Michael J. Sailor, Gael Gautier, and Leigh T. Canham

Citation: Applied Physics Letters **108**, 153111 (2016); doi: 10.1063/1.4947084
View online: http://dx.doi.org/10.1063/1.4947084
View Table of Contents: http://scitation.aip.org/content/aip/journal/apl/108/15?ver=pdfcov
Published by the AIP Publishing

Enhanced quantum yield of photoluminescent porous silicon prepared by supercritical drying

Jinmyoung Joo,[1,2,a)] Thomas Defforge,[3,a)] Armando Loni,[4,a)] Dokyoung Kim,[1] Z. Y. Li,[5] Michael J. Sailor,[1,b)] Gael Gautier,[3,b)] and Leigh T. Canham[4,5,b)]

[1]*Department of Chemistry and Biochemistry, University of California, San Diego, La Jolla, California 92093, USA*

[2]*Biomedical Engineering Research Center, Asan Institute for Life Sciences, Asan Medical Center, University of Ulsan College of Medicine, Seoul 05505, Republic of Korea*

[3]*Universite Francois Rabelais de Tours, CNRS CEA, INSA-CVL, GREMAN UMR 7347, 37071 Tours Cedex 2, France*

[4]*pSiMedica Ltd., Malvern Hills Science Park, Geraldine Road, Malvern, Worcestershire WR14 3SZ, United Kingdom*

[5]*Nanoscale Physics Research Laboratory, School of Physics and Astronomy, University of Birmingham, Edgbaston, Birmingham B15 2TT, United Kingdom*

(Received 9 February 2016; accepted 6 April 2016; published online 15 April 2016)

The effect of supercritical drying (SCD) on the preparation of porous silicon (pSi) powders has been investigated in terms of photoluminescence (PL) efficiency. Since the pSi contains closely spaced and possibly interconnected Si nanocrystals (<5 nm), pore collapse and morphological changes within the nanocrystalline structure after common drying processes can affect PL efficiency. We report the highly beneficial effects of using SCD for preparation of photoluminescent pSi powders. Significantly higher surface areas and pore volumes have been realized by utilizing SCD (with CO_2 solvent) instead of air-drying. Correspondingly, the pSi powders better retain the porous structure and the nano-sized silicon grains, thus minimizing the formation of non-radiative defects during liquid evaporation (air drying). The SCD process also minimizes capillary-stress induced contact of neighboring nanocrystals, resulting in lower exciton migration levels within the network. A significant enhancement of the PL quantum yield (>32% at room temperature) has been achieved, prompting the need for further detailed studies to establish the dominant causes of such an improvement. *Published by AIP Publishing.* [http://dx.doi.org/10.1063/1.4947084]

In the 25 years since the discovery of room-temperature photoluminescence (PL) from porous silicon (pSi),[1] steady improvements in PL efficiency and stability have resulted in a growing interest in the photoluminescent properties of nanoscale silicon and its application in optoelectronic devices, solar cells, chemical sensing, biological labeling, and consumer care products.[2–14] Electrochemically etched pSi generates nanocrystalline silicon, and the green to near infrared PL properties have been widely investigated, with the so-called "S-band" emission likely to originate from band-to-band recombination of quantum-confined excitons.[15,16] Quantum yields (QYs) for this emission band of up to 23% have been reported for pSi films and nanoparticles[2,3] and even higher than 50% for isolated silicon nanocrystals.[4–7] Inter-nanoparticle energy transfer has been shown to be at least partly responsible for limiting the quantum yield of solid nanocrystalline silicon structures with closely packed nanocrystals of varying size.[17]

For many potential applications, pSi is utilized as a mesoporous powder rather than a porous layer attached to the parent substrate. However, obtaining pSi in powder form with high micropore content and large surface area has been challenging because capillary stress and surface tension effects during the drying process cause collapse of the porous framework, resulting in loss of mechanical integrity, surface area, and pore volume. This generates an increased number of non-radiative defects that lowers the photoluminescence QY substantially.[18,19] In addition to defect-mediated nonradiative carrier recombination, the QY of photoluminescent pSi is limited by weak exciton localization in the interconnected nanocrystalline silicon network. This is not an issue with isolated colloidal nanoparticles.[15]

A variety of strategies have been investigated to minimize fracture and shrinkage of highly porous structures during drying, and to improve the reproducibility of material properties.[20] Pore collapse and morphological changes associated with surface tension forces during solvent evaporation have been reduced through use of pentane as a solvent; however, this solvent carries concerns related to health and safety, and the drying-induced changes are not completely eliminated.[20–22] Supercritical drying (SCD) has been demonstrated as a powerful tool for achieving very high porosity and surface area for many mesoporous materials, including pSi.[19,22–24] The beneficial effect of the SCD process, in comparison with air-drying (AD), is mainly a higher degree of mechanical integrity being maintained within the etched pore structure during removal of the electrolyte/rinse solution. Residual electrolyte is gradually displaced from the pores with isopropanol and subsequently replaced with liquid CO_2, which is then taken through the critical point and subsequently vented as a gas to leave an intact mesoporous structure with extremely large surface area (>1000 m^2/g) and, where appropriate, high micropore content.[23]

[a)]J. Joo, T. Defforge, and A. Loni contributed equally to this work.
[b)]Authors to whom correspondence should be addressed. Electronic addresses: msailor@ucsd.edu; gael.gautier@univ-tours.fr; and lcanham@psivida.com.

In this letter, we report an investigation into the photoluminescent characteristics of pSi powders prepared by incorporating the SCD process. Since electrochemically etched pSi contains closely spaced and interconnected silicon nanocrystals (<5 nm), pore collapse and structural changes within the nanocrystalline matrix after air-drying may affect the PL properties. We propose that higher concentrations of non-radiative defects, higher exciton migration levels, and lower porosity, all caused by nanostructured pore collapse, can lower the PL QY of pSi; thus, a higher degree of structural integrity being maintained through SCD facilitates high QY of photoluminescent pSi powders.

The pSi layer was manufactured by electrochemical etching of a single crystal p-type Si wafer in hydrofluoric acid (30 wt. %) with sulfuric acid additive (38 wt. %). After anodization, the pSi layer was separated from the parent Si substrate by application of an additional anodization in dilute HF solution, and then the electrolyte was displaced by flushing with isopropanol (IPA) while avoiding exposure to air. The pSi powders (several microns to millimetre-sized) were thoroughly rinsed with IPA, stored in IPA, and subsequently divided for each drying process: air-drying or supercritical drying. For SCD, the pSi powders were transferred while wet to a supercritical drying chamber (K850 Critical point dryer, Quorum Technologies, Ltd.), this being immediately filled with liquid CO_2, followed by the standardized sequential procedure reported previously.[23] For air-drying (AD), the IPA was allowed to evaporate in ambient air.

X-ray diffraction (XRD) patterns were first analysed to investigate the crystallinity and the size of the Si nanocrystallites. The XRD spectra of both air-dried pSi (AD-pSi) and supercritically dried pSi (SCD-pSi) powders revealed intense peaks for Si (111), (220), and (311) planes (Fig. 1(a)). The diffraction peaks of the AD-pSi sample were broader than the SCD-pSi sample; this suggests that the mean Si crystallite size in AD-pSi is slightly smaller than that of SCD-pSi according to the Scherrer equation.[25] The Raman spectra also support the conclusion that crystallite size in AD-pSi is smaller. The first-order Raman peak from crystalline silicon in the AD-pSi sample was broadened and shifted to lower energy compared to the SCD-pSi sample, consistent with a reduction in average crystallite size upon air-drying.[26] Using the model of Campbell and Fauchet,[27] the average particle sizes based on the Raman data are 2.5 nm and 3.7 nm for AD-pSi and SCD-pSi, respectively. However, the above interpretation is confounded somewhat by the known effects of lattice strain on XRD and Raman data.[24,28]

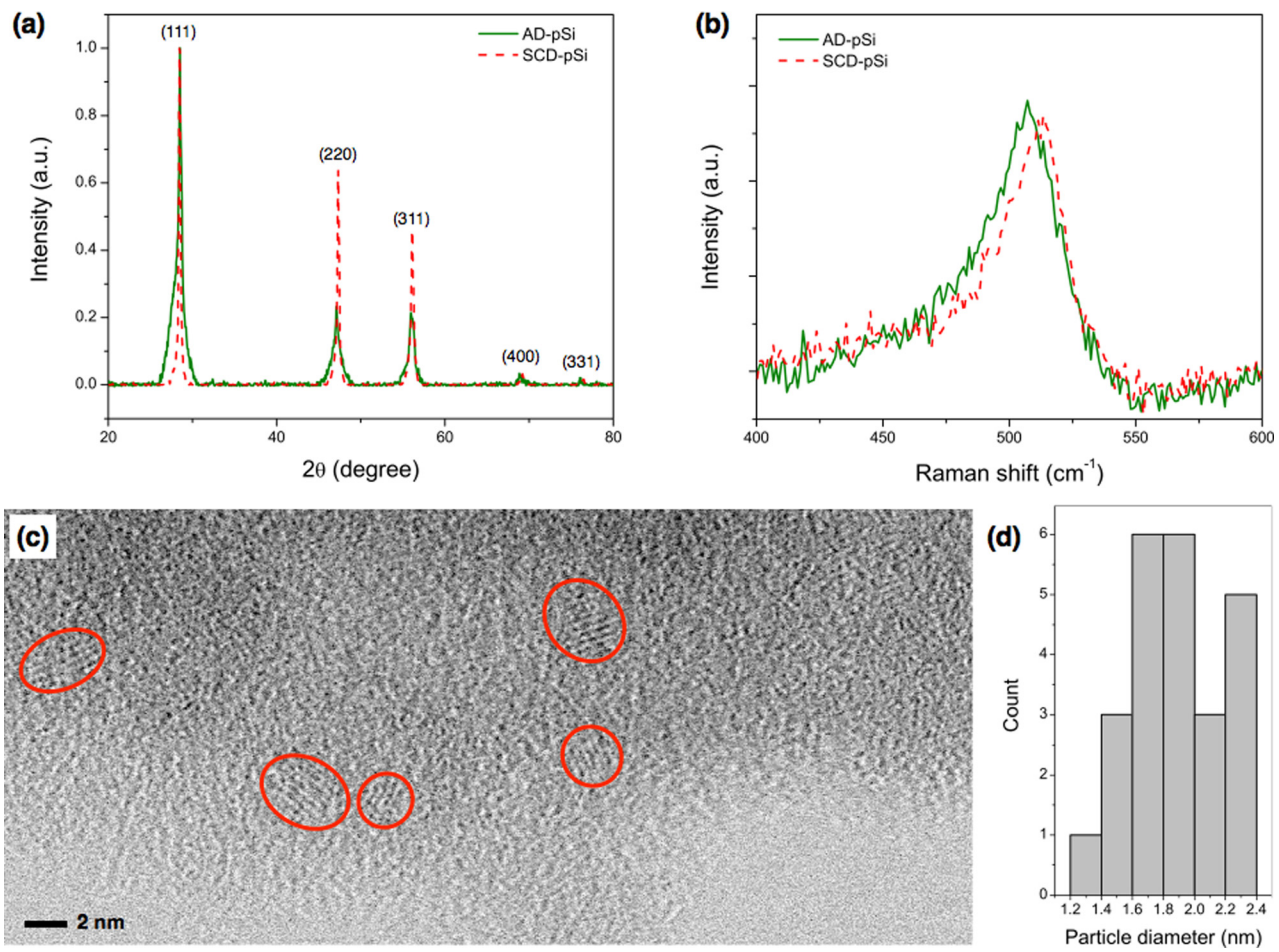

FIG. 1. (a) X-ray diffraction (XRD) spectra of pSi powders. The intensity is normalized to the Si (111) reflection. Green solid line: AD-pSi, red dashed line: SCD-pSi. (b) Raman spectra of pSi powders measured relative to a 785 nm laser line, at room-temperature. Si standard: 520.5 cm^{-1}; AD-pSi: 507.3 cm^{-1}; SCD-pSi: 513.6 cm^{-1}. (c) Bright field (BF) image of AC-STEM of a representative SCD-pSi (red circles indicate nanocrystalline silicon), and (d) corresponding nanocrystalline particle size distribution obtained by Feret diameter analysis of the BF-STEM images using ImageJ.[29]

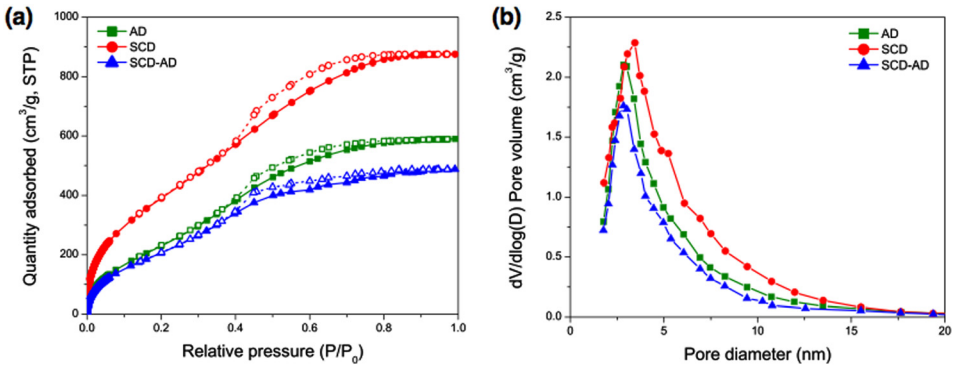

FIG. 2. (a) Nitrogen gas adsorption-desorption isotherm and (b) BJH (method of Brunauer, Emmet, and Teller) pore size distribution for pSi powders obtained from different drying processes: Air-drying (AD) and supercritical-drying (SCD) of as-etched pSi powders, and air-drying of re-wetted SCD-pSi powders in IPA (SCD-AD).

In order to characterize the size and size distribution of isolated silicon nanocrystallites prepared by SCD, a representative SCD-pSi sample was subjected to mechanical grinding between two highly polished silicon wafers, and then blown off the wafer surface directly onto a copper grid using a nitrogen gun. Aberration corrected scanning transmission electron microscopy (AC-STEM) analysis (JEOL 200 kV JEM2100F equipped with a CEOS probe corrector) revealed various shapes and sizes of silicon nanocrystals (Figs. 1(c) and 1(d)), although no nanocrystalline skeleton dimensions larger than about 2.5 nm in size were observed. This provides evidence of a tight size distribution of the SCD silicon nanocrystals, which can be expected to minimize the effects of exciton migration on PL quantum yield.[30,31]

Nitrogen gas adsorption/desorption analysis was conducted to determine surface area, pore volume, and average pore diameter for each powder obtained from the different drying processes (Fig. 2). Most notable is the substantially larger specific surface area per unit mass (1150 m^2/g) realized by utilizing SCD instead of AD (cf. 748 m^2/g), consistent with our previous study.[23] Analysis of the adsorption data revealed a correspondingly higher pore volume ($>1\,cm^3/g$) and larger average pore size ($\sim$3.3 nm) for SCD-pSi. This result also indicates a higher degree of mesoporosity has been maintained compared with AD-pSi (pore volume: $\sim$0.7 cm^3/g, pore size: $\sim$2.7 nm). To confirm the ability of SCD to retain higher surface area in the pSi powders, the SCD-pSi powder was re-wetted in IPA and then dried in air; this caused reductions in both surface area (671 m^2/g) and pore volume (0.6 cm^3/g), in a consistent manner. One can assume, therefore, that structural integrity is maintained for SCD-pSi powders due to the ability of SCD to avoid the enormous capillary forces generated at a typical liquid-vapour interface.

The PL measurements for pSi powders were conducted in ambient conditions. The excitation source was a UV LED (light emitting diode) ($\lambda_{ex} = 365$ nm, Ocean Optics). The absorption and emission spectra were obtained using an absolute measurement setup equipped with an integrating sphere (Labsphere, NH, USA) and a spectrometer (QE Pro, Ocean Optics). The emission spectrum of AD-pSi shows an approximate 2-fold lower intensity in comparable absorption ranges with that of SCD-pSi (Fig. 3). The absolute PL quantum yield of SCD-pSi powder was found to be 32.1%, while significantly reduced quantum yield (17.5%) was observed for AD-pSi (Table I). In addition, the quantum yield of the re-wetted SCD-pSi after air-drying (SCD-AD-pSi) decreased to 15.8%, which is comparable with the AD-pSi. The PL emission spectra of SCD-AD-pSi and AD-pSi were also comparable (Fig. 3). The slight blue shift (λ_{max}: 685 nm $\rightarrow$ 660 nm) observed in the PL spectrum can be a result of either (1) decreased size of quantum-confined nanocrystalline silicon domains consistent with the XRD and Raman analysis or (2) structural disorder and stress affecting the PL peak position.[24,28,32]

It is noted from Table I that while the quantum yield is significantly raised with supercritical drying, the FWHM is not dramatically narrowed. This latter observation has similarities to a previous study on size purification of isolated nanoparticles where, for example, narrow fractions (e.g., 1.31 ± 0.24 nm) gave rise to only minor improvements in FWHM.[34] A clue might come from spectroscopic measurements of single silicon nanocrystals, where oxide passivation layer thickness was reported to have a dramatic effect on luminescence linewidth.[35] Here, the homogeneous linewidth for specific chemical passivations appears to set a lower limit on linewidth improvements that can be expected by narrowing the size distribution. In addition, for interconnected nanocrystals, if collapsed larger parts of the air-dried skeleton are virtually non-luminescent, then the FWHM of photoluminescence may not be substantially broadened as a result of choice of drying technique.

We next compared the PL decay dynamics of samples subjected to the different drying processes. The emission

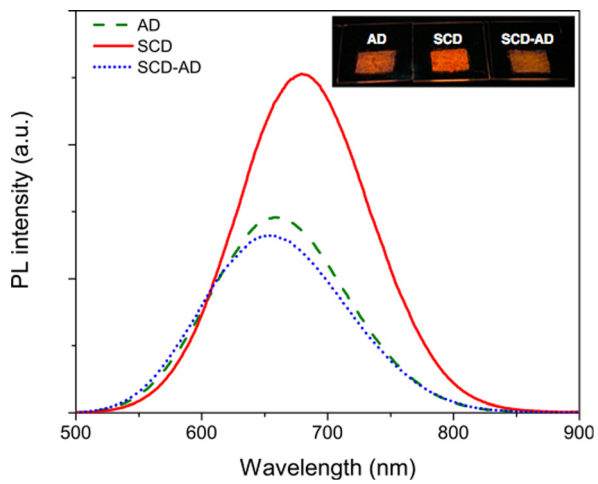

FIG. 3. Photoluminescence (PL) spectra ($\lambda_{ex} = 365$ nm, excitation intensity variation was <3% between each sample) of pSi powders obtained from different drying processes: Air-drying (AD) and supercritical-drying (SCD) of as-etched pSi powders, and air-drying of re-wetted SCD-pSi powders in IPA (SCD-AD). Inset: Photograph of the emission of corresponding pSi powders under UV excitation at room-temperature (taken with 460 nm long-pass filter to remove $\lambda_{ex} = 365$ nm excitation light).

TABLE I. Absolute quantum yield of pSi powders prepared by different drying processes.[a]

Sample type	AD-pSi	SCD-pSi	SCD-AD-pSi
Quantum yield (%)	17.5 ± 2	32.1 ± 2	15.8 ± 3
λ_{max} (nm)	660 ± 3	685 ± 3	657 ± 4
FWHM	127 ± 3	121 ± 2	129 ± 3

[a]AD-pSi is air-dried porous Si, SCD-pSi is supercritically dried porous Si, and SCD-AD-pSi is supercritically dried pSi that was then re-wetted with isopropanol and air-dried, as described in the text. Excitation wavelength is $\lambda_{ex} = 365$ nm. λ_{max} is the wavelength where the PL emission intensity is maximum. Full width at half maximum (FWHM) is obtained from a Gaussian fit, as an approximation of the inhomogeneous broadening associated with the ensemble of silicon nanocrystallites comprising the porous matrix.[33]

TABLE II. PL decay time constant (τ) of pSi prepared by different drying process ($\lambda_{ex} = 365$ nm). The time constant values are obtained from the normalized PL intensity-time trace in Fig. 4 fitted to first-order exponential function. Standard deviations of each time constant in multiple experimental measurements ($n > 3$) are less than 1.5 μs.

	Wavelength (nm)	AD-pSi	SCD-pSi	SCD-AD-pSi
τ (μs)	600	15.1	19.5	14.8
	650	24.6	31.9	23.8
	700	36.5	41.9	35.5
	750	47.6	54.3	44.3
	800	57.1	64.8	55.4

decays for all the samples studied here were found to fit reasonably well to an exponential function.[33] As seen previously for porous Si, the decay time constants (τ) were on the order of tens of microseconds, and each sample showed a pronounced increase in τ with increasing emission wavelength, in accordance with the quantum-confinement model (Fig. 4 and Table II).[15] Notably, the AD-pSi and SCD-AD-pSi samples displayed somewhat smaller emission decay lifetimes compared to SCD-pSi at each PL wavelength, consistent with the lower quantum yields observed for samples subjected to air-drying.

The superior quantum yield and longer excited state lifetime observed for SCD-pSi are attributed to lower structural disorder and fewer non-radiative defects, combined with a tight crystalline size distribution. It has been shown that structural disorder and stress in air-dried materials affect photoluminescence characteristics by formation of surface-related non-radiative recombination centers.[19,24] The gas adsorption data show that the AD process induced a loss of surface area and a decrease in pore volume consistent with collapse of the silicon nanostructure.[23] We conclude that the reduced PL quantum yield in air-dried nanocrystalline silicon potentially derives from an increase in non-radiative defects at the surface of the silicon skeleton; the escape of excitons via the interconnected nanocrystalline silicon network; and higher total internal reflections due to higher refractive index (lower pore volume). Reduced exciton localization in interconnected quantum-confined Si nanocrystals has been suggested as an important factor,[2] and the present results indicate that exciton migration into neighbouring Si nanocrystals is highly probable in AD-pSi. The fact that the air-dried samples are exposed to oxygen implies that their surface may become oxidized during the drying process. Oxidation-derived passivation of surface defects is known to reduce non-radiative recombination and increase QY on these types of samples,[3,33,36,37] so any differences in surface oxidation are apparently not as important in the present samples.

Based on these results, the beneficial effect of using supercritical drying for the preparation of pSi powders with enhanced photoluminescent properties is clear. Another important factor that may have some bearing on how the PL properties can be improved is how the pSi is stored after fabrication.[38] Specifically, it has been shown that the PL efficiency increases with storage time in ethanol solution.[29] In the present study, samples were stored in IPA between anodization and drying (SCD or AD) process, and like-for-like comparison must take the storage conditions into account. Moreover, complete removal of any residual toxic components or solvent from the pores while retaining an intact porous structure (with high surface area) and high PL quantum yield is important for many potential applications: e.g., loading of therapeutic molecules in biodegradable pSi for drug delivery and for tracking *in vivo*. Improved gas adsorption properties obtained herein with SCD indicate that a greater degree of physical integrity has been maintained during the drying process. The SCD process requires more expense

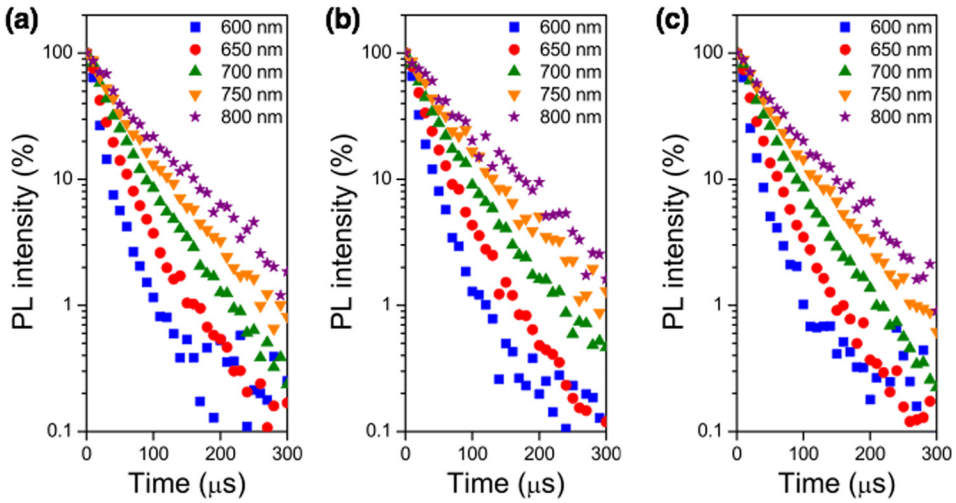

FIG. 4. Normalized PL intensity-time trace at different emission wavelength after pulsed excitation ($\lambda_{ex} = 365$ nm): (a) AD-pSi, (b) SCD-pSi, and (c) SCD-AD-pSi.

than AD to manufacture but is likely to be very important for material optimization in many high-value applications.

In summary, the benefits associated with the use of SCD, in comparison with conventional air-drying, for preparing photoluminescent pSi powders with extremely high surface area (>1000 m^2/g) have been demonstrated. The PL intensity and QY of as-etched pSi powders are significantly enhanced by employment of the SCD process. The PL QY of SCD-pSi is achieved up to 32%, which is ~two-fold higher compared with that of AD-pSi. Maintaining both a narrow size distribution for interconnected nanocrystals and a low concentration of non-radiative interfacial defects after the drying process is thought to be responsible for this advance with regard to pSi. The SCD process is a practical and promising approach for producing highly photoluminescent pSi materials.

This work was supported by the Defence Advanced Research Projects Agency (DARPA) under Cooperative Agreement HR0011-13-2-0017. The content of the information within this document does not necessarily reflect the position or the policy of the Government. The AC-STEM instrument employed in this research was obtained through the Birmingham Science City project "Creating and characterizing next generation advanced materials," supported by Advantage West Midlands and in part funded by the European Regional Development Fund.

[1]L. T. Canham, Appl. Phys. Lett. **57**(10), 1046 (1990).
[2]B. Gelloz, A. Kojima, and N. Koshida, Appl. Phys. Lett. **87**(3), 031107 (2005).
[3]J. Joo, J. F. Cruz, S. Vijayakumar, J. Grondek, and M. J. Sailor, Adv. Funct. Mater. **24**(36), 5688 (2014).
[4]J. Rinck, D. Schray, C. Kubel, A. K. Powell, and G. A. Ozin, Small **11**(3), 335 (2015).
[5]D. Jurbergs, E. Rogojina, L. Mangolini, and U. Kortshagen, Appl. Phys. Lett. **88**(23), 233116 (2006).
[6]F. Sangghaleh, I. Sychugov, Z. Y. Yang, J. G. C. Veinot, and J. Linnros, ACS Nano **9**(7), 7097 (2015).
[7]B. Cho, S. Baek, H. G. Woo, and H. Sohn, J. Nanosci. Nanotechnol. **14**(8), 5868 (2014).
[8]M. J. Sailor and E. C. Wu, Adv. Funct. Mater. **19**(20), 3195 (2009).
[9]R. J. Walters, G. I. Bourianoff, and H. A. Atwater, Nat. Mater. **4**(2), 143 (2005).
[10]Z. Z. Yuan, G. Pucker, A. Marconi, F. Sgrignuoli, A. Anopchenko, Y. Jestin, L. Ferrario, P. Bellutti, and L. Pavesi, Sol. Energy Mater. Sol. C **95**(4), 1224 (2011).
[11]J. Joo, X. Y. Liu, V. R. Kotamraju, E. Ruoslahti, Y. Nam, and M. J. Sailor, ACS Nano **9**(6), 6233 (2015).
[12]K. J. Nash, P. D. J. Calcott, L. T. Canham, M. J. Kane, and D. Brumhead, J. Lumin. **60**(1), 297 (1994).
[13]L. Gu, D. J. Hall, Z. T. Qin, E. Anglin, J. Joo, D. J. Mooney, S. B. Howell, and M. J. Sailor, Nat. Commun. **4**, 2326 (2013).
[14]J. H. Park, L. Gu, G. von Maltzahn, E. Ruoslahti, S. N. Bhatia, and M. J. Sailor, Nat. Mater. **8**(4), 331 (2009).
[15]A. Sa'ar, J. Nanophotonics **3**, 032501 (2009).
[16]M. V. Wolkin, J. Jorne, P. M. Fauchet, G. Allan, and C. Delerue, Phys. Rev. Lett. **82**(1), 197 (1999).
[17]R. Limpens and T. Gregorkiewicz, J. Appl. Phys. **114**(7), 074304 (2013).
[18]G. Amato, V. Bullara, N. Brunetto, and L. Boarino, Thin Solid Films **276**(1–2), 204 (1996).
[19]L. T. Canham, A. G. Cullis, C. Pickering, O. D. Dosser, T. I. Cox, and T. P. Lynch, Nature **368**(6467), 133 (1994).
[20]L. Canham, *Handbook of Porous Silicon* (Springer, 2014).
[21]C. J. Oton, Z. Gaburro, M. Ghulinyan, L. Pancheri, P. Bettotti, L. Dal Negro, and L. Pavesi, Appl. Phys. Lett. **81**(26), 4919 (2002).
[22]D. Bellet and L. T. Canham, Adv. Mater. **10**(6), 487 (1998).
[23]A. Loni, L. T. Canham, T. Defforge, and G. Gautier, ECS J. Solid State Sci. **4**(8), P289 (2015).
[24]K. W. Kolasinski, J. C. Barnard, S. Ganguly, L. Koker, A. Wellner, M. Aindow, R. E. Palmer, C. N. Field, P. A. Hamley, and M. Poliakoff, J. Appl. Phys. **88**(5), 2472 (2000).
[25]J. I. Langford and A. J. C. Wilson, J. Appl. Crystallogr. **11**, 102 (1978).
[26]Z. F. Sui, P. P. Leong, I. P. Herman, G. S. Higashi, and H. Temkin, Appl. Phys. Lett. **60**(17), 2086 (1992).
[27]I. H. Campbell and P. M. Fauchet, Solid State Commun. **58**(10), 739 (1986).
[28]M. Miu, M. Danila, I. Kleps, A. Bragaru, and M. Simion, J. Nanosci. Nanotechnol. **11**(10), 9136 (2011).
[29]H. G. Merkus, *Particle Size Measurements: Fundamentals, Practice, Quality* (Springer, Netherlands, 2009).
[30]S. Gardelis, A. G. Nassiopoulou, N. Vouroutzis, and N. Frangis, J. Appl. Phys. **105**(11), 113509 (2009).
[31]K. Furuta, M. Fujii, H. Sugimoto, and K. Imakita, J. Phys. Chem. Lett. **6**(14), 2761 (2015).
[32]K. Kusova, L. Ondic, E. Klimesova, K. Herynkova, I. Pelant, S. Danis, J. Valenta, M. Gallart, M. Ziegler, B. Honerlage, and P. Gilliot, Appl. Phys. Lett. **101**(14), 143101 (2012).
[33]K. Matsumoto, R. Nishio, T. Nomura, K. Kamiya, M. Inada, and S. Suzuki, Jpn. J. Appl. Phys., Part 1 **54**(2), 021301 (2015).
[34]M. L. Mastronardi, F. Maier-Flaig, D. Faulkner, E. J. Henderson, C. Kübel, U. Lemmer, and G. A. Ozin, Nano Lett. **12**(1), 337 (2012).
[35]I. Sychugov, A. Fucikova, F. Pevere, Z. Yang, J. G. C. Veinot, and J. Linnros, ACS Photonics **1**(10), 998 (2014).
[36]V. Petrova-Koch, T. Muschik, A. Kux, B. K. Meyer, F. Koch, and V. Lehmann, Appl. Phys. Lett. **61**(8), 943 (1992).
[37]G. Ledoux, J. Gong, and F. Huisken, Appl. Phys. Lett. **79**(24), 4028 (2001).
[38]See supplementary material at http://dx.doi.org/10.1063/1.4947084 for the experimental details.